Viktor Krechik[2], Stanislav Myslenkov[1,2,3*], Maria Kapustina[2]
[1] Lomonosov Moscow State University, Moscow, Russia
[2] Shirshov Institute of Oceanology, Russian Academy of Sciences, Moscow, Russia
[3] Hydrometeorological Research Centre of the Russian Federation, Marine forecast division, Moscow, Russia
***Corresponding author:** stasocean@gmail.com

NEW POSSIBILITIES IN THE STUDY OF COASTAL UPWELLINGS IN THE SOUTHEASTERN BALTIC SEA WITH USING THERMISTOR CHAIN

ABSTRACT. The article gives an analysis of a unique data of the thermistor chain, which installed on the D-6 oil platform in the coastal zone of the Baltic Sea. In total 10 temperature sensors were installed at different depths with a recording interval of 1 min, the depth at the installation site was 29 m. Based on satellite data, ship measurements and thermistor chain observation the characteristics and dynamics of the sharp decrease in water temperature which registered in the south-eastern Baltic Sea (Gdansk Bay area), during June 5-12, 2016 are analyzed. The temperature decreasing caused by the simultaneous action of at least two factors: wind-driven Ekman upwelling and advection of cold water. Scales of temporal and spatial variability of water temperature in a coastal zone of the south-eastern Baltic Sea near the coast of the Kaliningrad region are described. This event led to the considerable SST (sea surface temperature) drop by more than 8 °C for two days. The rate of reduction of its temperature during certain upwelling periods can reach 0.3-0.4 °C per hour, but the maximum warming rate between phases varies from 0.25 to 0.28 °C per hour. This dramatically changed the conditions of the thermal balance of the sea surface. The width of the upwelling, as seen in the SST data, was about 25 km. Satellite data were supplemented with data of a thermistor chain and CTD measurements. The high correlation between water temperature variability and changes in wind parameters: when the wind speed has decreased and its direction has changed, the response of the vertical thermal structure has occurred very quickly, sometimes within 1 hour. Thermistor chain data allow to evaluate the vertical temperature distribution and get more detailed analysis of temporal variability and short pulsations of upwelling.

KEY WORDS: coastal water; SST; satellite data; wind; Baltic Sea; upwelling; thermistor chain

CITATION: Viktor Krechik, Stanislav Myslenkov, Maria Kapustina (2019) New possibilities in the study of coastal upwellings in the southeastern Baltic Sea with using thermistor chain. Geography, Environment, Sustainability, Vol.12, No 2, p. 44-61
DOI-10.24057/2071-9388-2018-67

INTRODUCTION

Coastal upwelling is one of the most significant factors in the variability of surface water temperature near the coast (Kahru et al. 1995), and the most important vertical water exchange mechanism in the coastal zone of the sea (Esiukova et al. 2017; Hela 1976). In the conditions of two-layer stratification that is typical for the Baltic Sea, this phenomenon plays a key role in the balance of nutrients within the upper layer of the water column (Svansson 1975). In addition, after the first spring phytoplankton bloom, when the nutrients in the surface layer are depleted, coastal upwelling is sufficient to maintain the bloom (Siegel et al. 1999).

The first documented scientific observation of the effect of upwelling on the properties of the surface layer in the Baltic Sea was performed by Alexander von Humboldt in 1834 (Leppäranta and Myrberg 2010). In the second half of the 20th century observations of the temperature variability in the coastal zone were carried out on the basis of instrumental measurements and were of a local nature (Simons 1978; Walin 1972). A new stage in the study of sea surface temperature (hereafter SST) and upwelling began in the late 1980s when remote sensing data became widely used. During this period, a lot of studies of bioproductivity and upwelling phenomena were performed on the basis of satellite images of the Baltic Sea area (Horstmann 1983; Bychkova and Viktorov 1987; Gidhagen 1987). Later, when a large array of sea surface temperature maps was accumulated, statistical work on SST appeared both for the entire Baltic Sea (Lehmann and Myrberg 2008; Lehmann et al. 2012) and for its regions (Kreżel et al. 2005; Kowalewski and Ostrowski 2005).

Coastal upwelling within the investigated area occurs quite often (Bychkova et al. 1988; Lehmann et al. 2012; Kozlov et al. 2012) and is observed during the northern, northeastern and eastern winds (Kowalewski and Ostrowski 2005). From 2000 to 2014 135 upwelling events that occurred in the studied area during the period of stable thermal stratification (May-October) were identified (Esiukova et al. 2017).

Thus, satellite data are effectively used to detect and study upwelling. Their big advantage is a large spatial coverage. However, there are a number of shortcomings. Firstly, due to the high cloudiness typical of certain seasons for the Baltic Sea, these data are very irregular in time (Zhelezova et al. 2018). Secondly, satellite images may only provide a representation of a thin surface layer, and data about the state of water column deeper layers remains inaccessible (Elachi and van Zyr 2006).

Currently, the water temperature vertical structure in the Baltic Sea are mainly obtained when making sections with discrete oceanographic stations or using towed CTD-probes (Krechik and Gritsenko 2016; Kapustina et al. 2017; Demidov et al. 2011; Stepanova et al. 2015; Chubarenko et al. 2013; Demchenko and Chubarenko 2012; Zhurbas et al. 2012). In the southeastern part of the Baltic Sea, a large amount of such data are obtained during the research vessels' cruises and the industrial environmental monitoring of the Kravtsovskoye oil field (Sivkov et al. 2012). As part of the monitoring, measurements of meteorological characteristics are carried out on the D-6 platform (Stont et al. 2012), and measurements of waves and currents have been carried out periodically (Ambrosimov et al. 2013). Monitoring of the temperature and salinity is based on CTD measurements from the surface to the bottom once a month (Sivkov et al. 2012). Such data allow us to identify spatial heterogeneity, seasonal and inter-annual variability of water temperature.

The thermistor chains are used for investigation of the propagation parameters of internal waves and the high-frequency variability of water temperature (Gemmrich and van Haren 2002; Van Haren et al. 2005; Serebryanyy et al. 2014) and also to study different-scale effects of vertical mixing and stratification (Gemmrich and van Haren 2001; Brookes et al. 2013) all over the world.

Such method of observation is little used in the Baltic Sea (Massel 2015), but the studies which based on the thermistor chains data show good results and effectivity of these devices (Sellschopp 1991; Morozov et al. 2007; Van der Lee and Umlauf 2011).

There are first results of analysis data, which received from thermistor chain installed in southeastern part of the Baltic Sea on D-6 platform in 2015, presented in articles (Myslenkov et al. 2017a,b). The thermistor chain data allow us to study the vertical structure of the temperature distribution at different time scales, including the hourly scale (Myslenkov et al. 2017a). Comparison of in situ measurements with remote sensing data carried out for this region showed that the systematic error of satellite data did not exceed +0.25 °C in all cases and was no more than +0.14 °C when strong diurnal warming was not taken into account (Myslenkov et al. 2017b). Thus, our data set represents a rather rare occasion for the joint application of remote sensing data and in situ data to study upwelling.

The purpose of this study is to describe and analyze the upwelling parameters recorded in the summer of 2016 near the coast of the Kaliningrad region, based on satellite imagery and in situ measurements. New possibilities of using the thermistor chain in the study of upwelling are presented.

DATA AND METHODS

SST was obtained in the study area from the multi-sensor Earth remote sensing data, distributed by CMEMS (Copernicus Marine Environment Monitoring Service), with spatial resolution 0,02 * 0,02 degree and L3 processing level. This data were averaged daily. The data were obtained from different scanners: AVHRR/3 (MetOp-B, NOAA-18 and NOAA-19), MODIS (Terra and Aqua), VIIRS (Suomi NPP) and AMSR-2 (GCOM-W1). Non-corrected products are 24 hourly syntheses centered at 00 UTC. Quantum-GIS software was used to process and analyze the data.

For the joint analysis of satellite and thermistor chain data, the Level-2 SST images downloaded from NASA OceanColor website (https://oceancolor.gsfc.nasa.gov) were used. The analysis was carried out on the basis of data from spectroradiometers MODIS, based on the Terra and Aqua satellites, as well as the spectroradiometer VIIRS, based on the Suomi NPP satellite. The spatial resolution of the data was 1 km in the nadir for MODIS and 0.75 km in the nadir for VIIRS and the swath' width were 2330 and 3000 km, respectively. At the first stage, the images covered the thermistor chain location was selected, regardless of the position of the satellite track. Then the location of the satellite data points relative to the location of the measuring device was checked. The QGIS software was used for this procedure. The data points located from the thermistor chain at the distance exceeded the double spatial resolution of the MODIS spectroradiometer were not taken into account. At the second stage, the difference between the SST data and the temperature measured by the thermistor chain was calculated. Next, a filter based on the three sigma rule (Pukelsheim 1994) was applied. The author of the work (Lehmann 2013) showed that for gross measurement errors, which act randomly, this rule works poorly. For this reason, the confidence interval was reduced from 99.73 to 95%. The boundaries of the confidence interval were determined by the expression $X_{mean} \pm 1.96\sigma$.

The data of the thermistor chain which installed on the offshore ice-resistant fixed platform (hereafter OIFP) D-6 (Fig. 1) were used. D-6 is located in the coastal zone 22 km offshore of the Curonian Spit (Southeastern Baltic Sea). The thermistor chain consists of 10 "Starmon mini" sensors located at the depths of –0.9, 0.15, 1, 3, 5, 8, 10, 13, 24, 28 m. The depth at the installation site is 29 m. In the event of a strong wave, the first two-three sensors were periodically in the air, but these data can be filtered because of the sharp increase in the temperature dispersion. The time step of temperature measurements is 1 min; accuracy is +/- 0.025 °C.

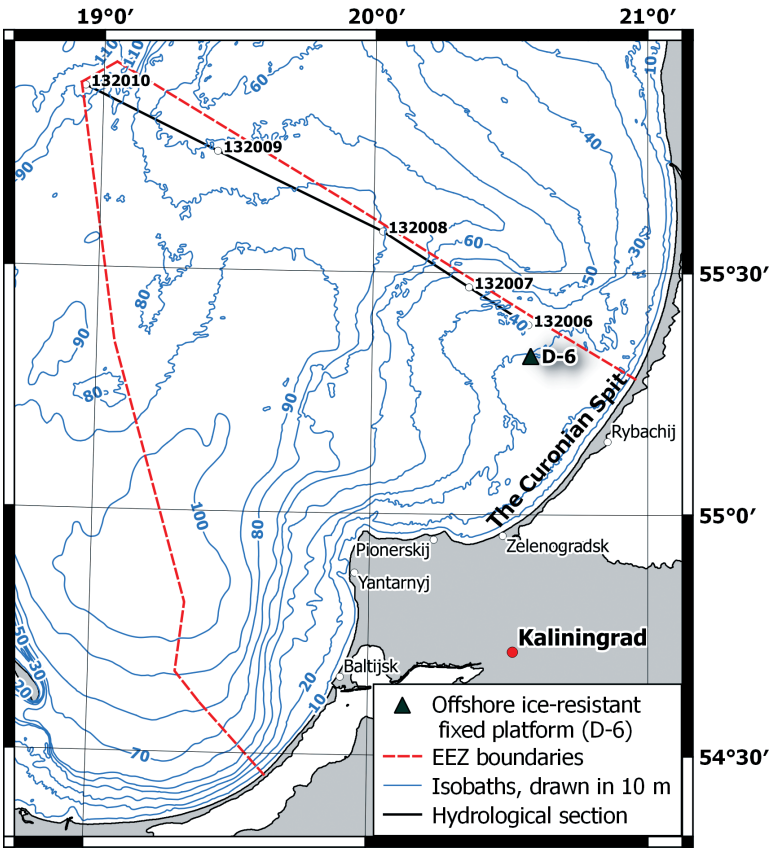

Fig. 1. The study area and stations location

The vertical temperature distribution on the hydrological section (stations 132006-132010, Fig. 1)) was measured using a CTD90M probe, produced by Sea & Sun Technology, Germany. The soundings were made from the surface to the bottom in the mode of the free sliding probe along the hawser. The lowering speed of the instrument was from 0.7 to 1 m/s with a measurement frequency of 4 Hz. This method makes it possible to record changes in the parameters with a high resolution. The measurements were carried out during the 132nd cruise of the research vessel Professor Shtokman (11-16 of June 2016).

Meteorological data were received by the meteorological station KRAMS-4-03, which is located on the OIFP D-6. The height of the sensors is 27 m above the sea. The station automatically measures and records the following parameters: air temperature and relative humidity, wind speed and direction, atmospheric pressure, cloud height, meteorological optical visibility range. Only data on wind speed and direction were used in this study.

Wind speed and direction data over the all study area were obtained from the high-resolution reanalysis NCEP/CFSR (Climate Forecast System Version 2) (2011-2016) (Saha et al. 2014; CISL... 2015). The wind's parameters were obtained at 10 meters height with a spatial resolution of ~ 0.2 °. To improve the quality of visualization, the data are presented with a spacing of ~0.4 ° and a time step of 3 hours.

RESULTS

All available sea temperature data (satellite, hydrological section) was used to study the sharp decrease in water temperature which had been observed since June 4 till

12, 2016 along the coast of the Curonian Spit. However, the basic information for analysis was obtained by the thermistor chain installed on the D-6 platform. According to these data, in May 2016 an intensive warming of the upper water layer was observed in the southeastern Baltic Sea. Thus, at the beginning of June, the water surface temperature was about 19–20 °C. At the same time the upper mixed layer (UML) thickness was not great, and at the depth of 13 m the temperature varies from 10 to 11 °C (Fig. 2). Since June 4 till 11, the surface temperature had been dropped to 8.2 °C and then, its values increased again to 20 °C by June 26. The amplitude of the temperature was more than 10 °C. It is the unique and extreme event for the summer period in this region. Due to the availability of high temporal resolution water temperature data at the different depths obtained by the moored thermistor chain, it became possible to make a deep analysis of this event.

In the coastal zone, similar temperature dropping is usually associated with upwelling (Lehmann and Myrberg 2008). However, it is well-known that a decrease in temperature could be caused by various reasons, such as atmospheric cooling effects, advection of colder waters and upwelling events (as wind-driven or eddy-driven). Apparently, in the studied case, the temperature decreasing could be caused by the simultaneous action of at least two factors from those, which listed above: wind-driven upwelling and advection. As far as upwelling is a complex dynamic process, it should be considered as a whole.

Let us consider a relatively short period of time since June 1 till 16, 2016 in more details. The water column had been well stratified and the surface layer temperature varied from 15.67 to 18.79 °C before the upwelling event started. At the time of the cooling started, the sea surface temperature at the observation point was 18.55 °C. Strong NNE wind, blowing since the last half of 3 till 5 of June caused the formation of an upper mixed layer. Simultaneously with changing of the wind direction to the northern, there was the temperature dropping, registered by the thermistor

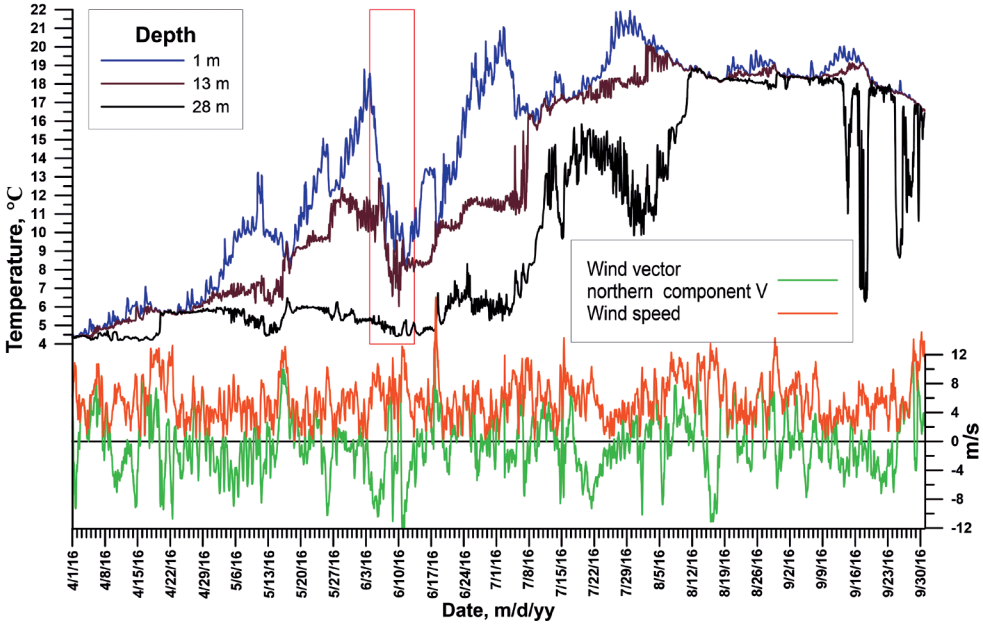

Fig. 2. The water temperature at the upper, medium and near-bottom layers according to the data of the thermistor chain during April 1–September 30, 2016, and the northern wind component and also wind speed according to NCEP/CFSR reanalysis near the D-6 platform. The red frame shows the period of the studied event

chain. By the end of June 5, UML thickness was about 10 m and the temperature decreased by 5.31 °C. The average cooling rate of the UML was about 0.1°C per hour. At the water depths of 24 and 28 m, no significant changes were recorded (Fig. 3).

The reaction of coastal waters in the study area on the wind direction changing was confirmed by remote sensing data. On the satellite image on June 6 the cold water jets were well-identified. The SST map showed three such regions: in the north of the study water area, along the Curonian Spit coast and near the western coast of Kaliningrad region (Fig. 4). Taking into account the direction of the wind, blowing along the coast, the presence of such jets is a typical occurrence of the Ekman origin upwelling event. The presence of different areas (from north to the south) where the same events have been recognized is evidence of this type of upwelling origin. It should be noted that a cold water jet pressed to the shore and observed in areas where the coast extends from north to south direction.

Due to the northern wind impact had been continued, the average rate of cooling of the water column increased to 0.16 °C per hour at the beginning of June 7. The thickness of the UML reached 13 m, and its temperature dropped to 9.6 °C. The temperature dropping has been lasting for 25 hours. Then the wind speed had decreased and at 2 am on June 7, the stratification began to recover. Later, the wind changed the direction to the west and water temperature started to increase (Fig. 3). On June 8 the values of water temperature started to show the recession again. The average rate of cooling was about 0.16 °C per hour. However, at this time, the southeastern wind was observed over the water area, which couldn't lead to the formation of coastal upwelling either under the forcing of the Ekman transport or the downsurge. This situation was also well demonstrated by the fact that there was no cold water in the surface layer along the western coast of the Kaliningrad region. Consequently, here we have seen no coastal upwelling, but rather the advection of a cold water stream from the neighbour water areas. Apparently, due to the long

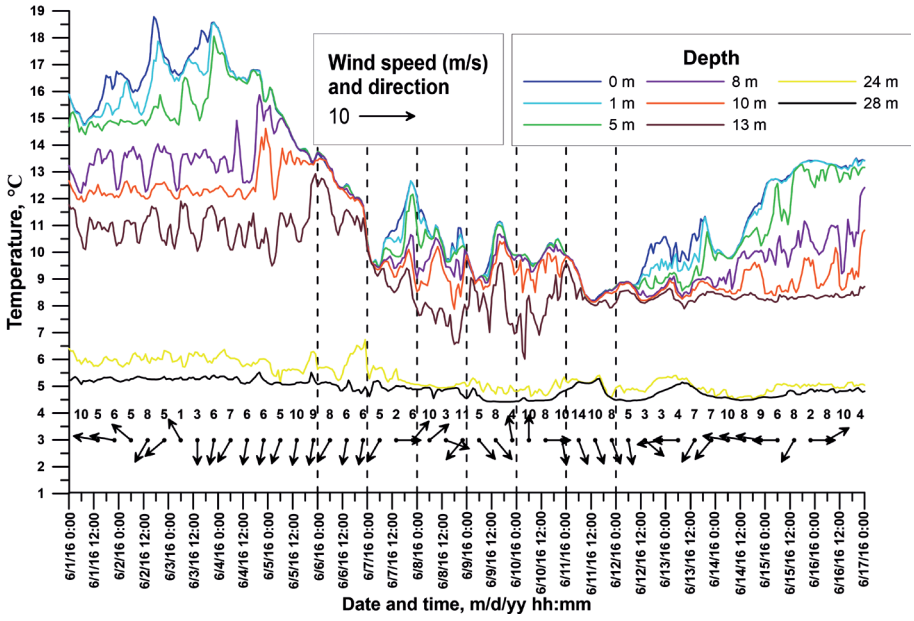

Fig. 3. The water temperature at different depths according to the data of the thermistor chain during 01-16.06.2016, and the wind speed and direction at the D-6 platform (marked every 8 hours). Intermittent vertical lines indicate the time of the shown satellite images

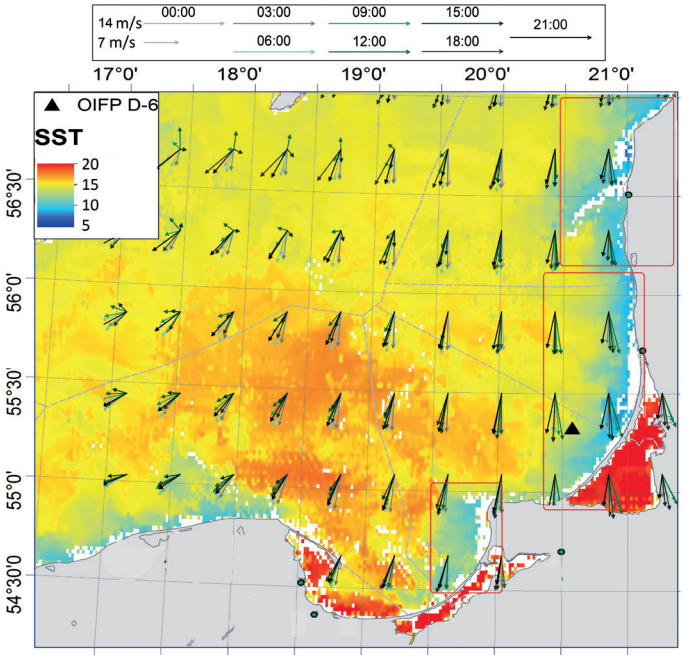

Fig. 4. Wind speed and direction (3 hourly arrows, NCEP/CSFR reanalysis) on June 5, 2016 and SST on June 6, 2016 (coloured contours with SST in °C, satellite data). Top panel: sample arrows indicating 14 m/s and 7 m/s winds, colour coded for the synoptic hours of observation. The red frames mark the locations of the Ekman origin upwelling event occurrence

exposure of the west and south-west winds in combination with the aspect of the coastline, a positive sea level anomaly was formed here. The coastal level anomaly caused the formation of a compensation off-shore current. This current began to deliver cold water in the south-western direction to the OIFP D-6 (Fig. 5).

On the night of June 9, the NE wind leads to the beginning of the second phase of upwelling. The thickness of the UML increased, and the SST decreased (Fig. 3). At 4 a.m. on June 9, the direction of the wind changed to the north-west and the upwelling stopped. The temperature of the surface layer increased. Thermal stratification appeared in the water column again (Fig. 3).

On June 10, the thermal stratification of the water column increased (Fig. 3). In the first half of the day a southerly wind was observed above the area, and then the direction of the wind veered to the west. From 7 p.m. the wind speed increased to 10-12 m/s and direction changed to northerly. This led to the beginning of the third phase of upwelling. Since the beginning of June 11, the temperature of the surface layer has been rapidly decreasing to 8.14 °C (11th of June at 10:54). The temperature decreased on average 0.13 °C per hour. Then its slow growth was noted (Fig. 3).

On June 11, because of the rather strong cloudiness above the Gdansk Basin, it was not possible to obtain a high-quality satellite image. However, we can recognize a decrease in the SST values of the open part of the sea. There was a noticeable increase in the area of coastal waters with lower temperatures north towards of the D-6 platform (Fig. 6).

The hydrological section performed in this period (Fig. 7) shows that the vertical temperature distribution in the Gdansk Basin consisted of two layers. The surface temperature of the open sea varies between 14-14.8 °C. In the coastal zone from an isobath of 50 m, where the upwelling

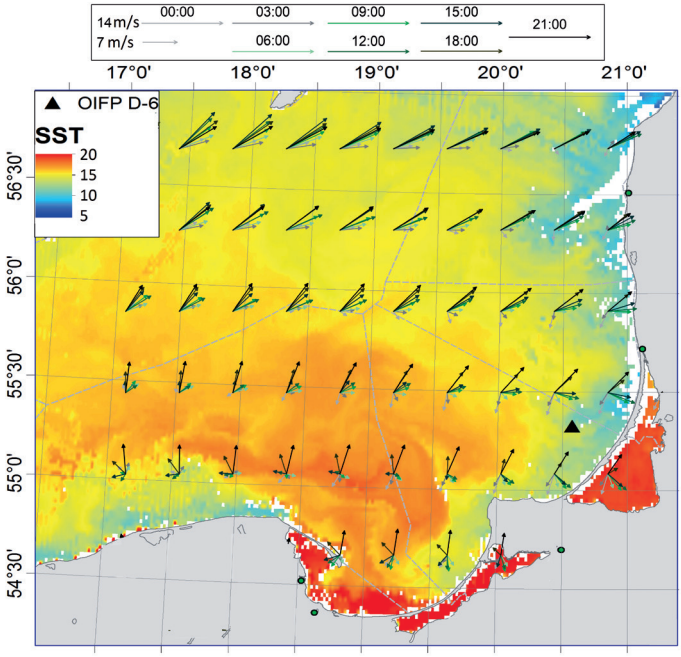

Fig. 5. Wind speed and direction (3 hourly arrows, NCEP/CSFR reanalysis) on June 7, 2016 and SST on June 8, 2016 (coloured contours with SST in °C, satellite data). Top panel: sample arrows indicating 14 m/s and 7 m/s winds, colour coded for the synoptic hours of observation

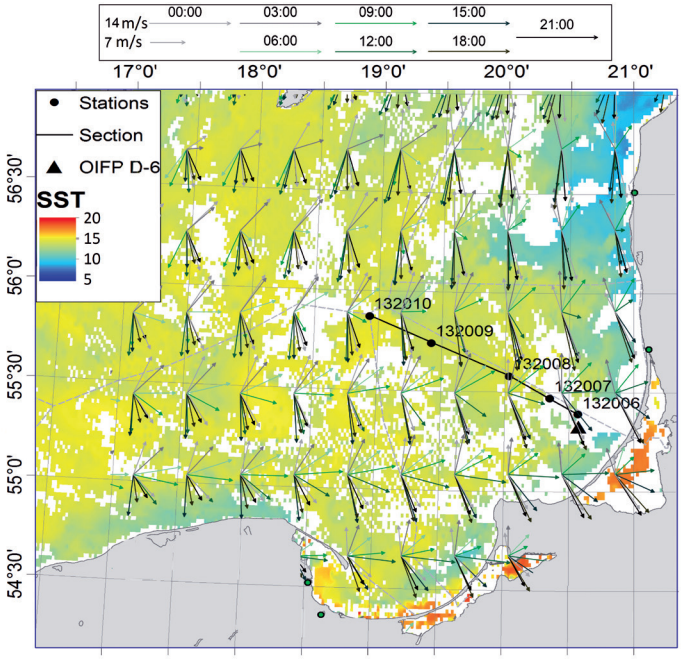

Fig. 6. Wind speed and direction (3 hourly arrows, NCEP/CSFR reanalysis) on June 10, 2016 and SST on June 11, 2016 (coloured contours with SST in °C, satellite data). Top panel: sample arrows indicating 14 m/s and 7 m/s winds, colour coded for the synoptic hours of observation

occurred, the surface layer temperature varied from 9.6 (station 132006) to 12.4 °C (station 132007). The upper boundary of the seasonal thermocline penetrated down to 18 m, and its thickness reduced from 14 to 8 m due to the rising of the upper part. Gradients in the thermocline core also decreased from 0.6-0.8 °C/m to 0.2-0.3 °C/m towards the shore.

According to the thermistor chain data, the upwelling in the study area lasted until 10 a.m. on June 12 (Fig. 3). Then the wind direction changed and the warming of the water column began. From June 12 10:00 onwards, SST (surface thermistor) reached values greater than 10 °C. Thermal stratification was well traced to a depth of 8 m. Below this depth, there was a quasihomogeneous layer, which thickness was more than 5 m. On June 13, the water column was thermally stratified in the same way. The surface layer had warmed up and at 7 p.m. on June 13 the SST values in the area of the D-6 platform increased to 11.36 °C. (Fig. 3). Then, under the influence of the northeast wind, the temperature dropped to 9.79 ºC on June 14 at 7:27 am. It should be noted that the reaction of the water column began only when the wind speed had increased up to 8 m/s. Despite the fact that the wind of the same direction at a speed of 5-7 m/s had been blowing during 6 hours over the water area before it. Then the warming up of the water continued and since the end of June 15 till the beginning of June 17, the temperature of the water column varied from 13.13 to 13.47 ºC (Fig. 3).

The processes described above could be characterized in some numerical indicators, such as the thickness of the UML, the sea surface temperature minimum and maximum, the rate of temperature variability, the weather and etc. The detailed description of the hydrometeorological conditions in the study area separately for each day is contained in Table1.

The information contained at Table 1 clearly demonstrates that in contrast to satellite data, the thermistor chain allows to estimate the vertical structure of water, as well as the dynamics of temperature changes during various events with a high resolution. At the same time, satellite data allows as to see the dynamics of coastal upwelling over a large water area and observe the same event on a different spatial and temporal scale. And meteorological data is critically necessary for the correct interpretation of remote sensing data and in-situ measurements.

DISCUSSION

Any research aimed at estimation and analyzing new possibilities, methods and techniques for studying natural phenomena should cover a number of questions dedicated to their effectiveness. One of

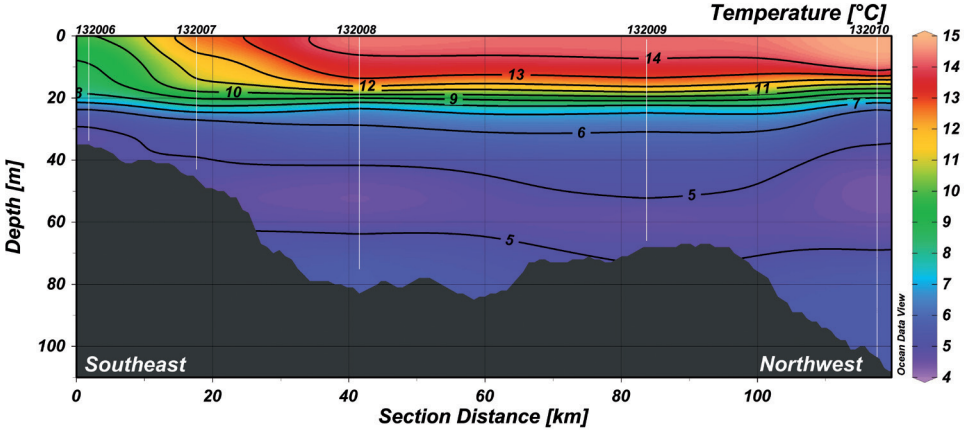

Fig. 7. Vertical temperature distribution on June 11 at the hydrological section. The location of the section is shown at Fig. 1 and Fig. 6

Table 1. Hydrometeorological conditions for the period from 5 to 13 of June 2016

Date (DD. MM)	Meteorological conditions	Characteristics of the surface layer					
		According to thermistor chain data (average temperature gradient)			According to remote sensing data		
		UML thickness	Temperature changes (for horizons 1 and 5 m.)	Average rate of temperature decreasing / increasing, (°C / hour) (1 and 5 m.)	SST of the open sea (°C)	SST of the upwelling zone (°C)	SST of the D6 platform area (°C)
5.06	NNE with speed 5-11 m/s (maximum at 3 p.m.)	Increasing from 5 m. to 8 m. (4 a.m.), than to 10 m. (7 p.m.)	Decreasing from 16 (0:00) to 13.3 °C (10 p.m.)	-0.11; -0.11	17-18	10-11	14-15
6.06	NNE, 3-13 m/s	10 m.	Decreasing from 13.5 °C (0:00) to 9.9 °C (11 p.m.)	-0.16; -0.17	16-17	9-10	13-14 (Fig. 4)
7.06	NNE, NE 2-5 m/s	13 m. (0:00-6 a.m.)	Increasing from 9.6 (0:00) to 12.6 °C (7 p.m.)	0.16; 0.16	15-16	10-11	12-13
7.06	From 11 a.m. direction changes to W-SW, 1-6 m/s	Up to 1 m. (7 a.m. - 6 p.m.)					
		5 m. (7 p.m.-11 p.m.)	Decreasing to 11.4 °C (11 p.m.)	-0.30; -0.34			
8.06	Till 12 p.m. SW, 7-10 m/s, than W, 2-8 m/s	Increasing from 5 m. (0:00-2 a.m.) to 8 m. (3 a.m.-8 a.m.), than to 10 m. (9 a.m.-2 p.m.)	Decreasing from 11.6 °C (0:00) to 9.9 °C (5 p.m.)	-0.15; -0.14	15-17	11-13	13 (Fig. 5)
8.06	From 6 p.m. NNE, 7-13 m/s	Decreasing to 5 m. (3 p.m.-11 p.m.). Increasing to 8 m (9 p.m.), than - 10 m.	Decreasing to 9.5 °C (11 p.m.)	-0.08; -0.07			
9.06	To 4 a.m. NNE, 2-7 m/s.	10-13 m. (0:00 - 8 a.m.)	Decreasing from 9.3°C (0:00) to 8.9 °C (3 a.m.)	-0.21; -0.25	15	9-12	11-12
	From 5 a.m. NW-NNW, 5-8 m/s	8 m. (9 a.m.-3 p.m.),	Increasing from 8.9 °C (4 a.m.) to 11.1 °C (2 p.m.)	0.21; 0.21			
9.06	From 8 p.m. - S, 1-6 m/s	10 m. (4 p.m. - 11 p.m.)	Decreasing to 9.8 °C (at 11 p.m.)	-0.18; -0.18			

10.06	Till 11 a.m. S-SSW, 7-10 m/s	8 m.	Decreasing from 9.8°C (0:00) to 9.6°C (5 a.m.)	-0.05; -0.06	14-15	11-12	10-11
10.06	From 12 p.m. W-NW, up to 12 m/s.		Increasing from 9.6 °C (at 6 a.m.) to 10.5 °C (6 p.m.)	0.08; 0.08			
	From 7 p.m.-N, 9-12 m/s.		Decreasing from 10.4°C (7 p.m.) to 9.8°C (11 p.m.)	-0.14; -0.14			
11.06	NNW-N, 9-14 m/s	10 m. (0:00-6 a.m.)	Decreasing from 9.8 °C (at 0:00) to 8.2 °C (at 11 a.m.).	-0.12; -0.13	13-14	11	12 (Fig. 6)
		13 m. (7 a.m.-5 p.m.), than 10 m. (6 p.m.-11 p.m.)	Increasing to 8.8°C (11 p.m.)	0.05; 0.06			
12.06	NW-NNW, 3-7 m/s	Decreasing from 13 m. (0:00-10 a.m.) to 0 m. (11 a.m.-11 p.m.)	Increasing from 8.8 °C (at 0:00) to 10.5°C (at 10 p.m.)	0.06; 0.03	13-14	10-11	11
12.06	At 7 p.m. NNE-E, 1-3 m/s.						
13.06	ENE-E, 3-4 m/s	0 m.	Decreasing from 10.6 °C (at 0:00) to 9.7 °C (at 9 a.m.)	-0.08; -0.03	14-15	12-13	11-12
13.06	From 10 a.m. direction changes to NNE -NE, 7-8 m/s	1-5 m. (4 p.m.-11 p.m.)	Increasing to 11.3°C (5 p.m.)	0.10; 0.18			

the main objectives of similar studies is the validation of new and generally accepted methods and the estimation of the difference between their results. The idea of comparing remote satellite data with contact measurements is not new. However, in the framework of this study the joint analysis of different time scale data was performed. We have made validation of the satellite data with the thermistor chain data. To increase the time resolution of the remote sensing data the information obtained by three different satellites was analyzed. The preliminary data set included not only the acquisition data received directly over the OIFP (2 times a day) but also images containing SST data near the D-6 platform. It is known that the spatial resolution of satellite data deteriorates from the nadir to the edge of the swath. For this reason, we took into account the data in which the distance from the thermistor chain to the centre of the nearest pixel did not exceed 2 km. Then the second stage of data filtering was carried out. The procedure is described in detail in the "Materials and Methods" section. The statistical estimation of the data set is shown in Table 2, and the results of the data comparison are shown in Fig. 8.

The maximum statistical indicators values are shown in bold and the minimum one is shown in underline.

Table 2. The statistical estimate of the distance from the SST map value point to the point of the thermistor chain installation and the difference between the remote sensing data and in-situ measurements

Characteristic	Statistical indicator	Aqua	Terra	Suomi	All satellites
Distance from the OIFP to pixel center	Average	**1.03**	0.77	0.51	0.75
	Median	**1.04**	0.65	0.42	0.73
	Standard deviation	**0.42**	0.36	0.36	0.43
	Minimum	0.25	**0.4**	0.15	0.15
	Maximum	1.7	**1.83**	1.42	1.83
	Count	18	19	21	58
The difference between satellite and in-situ data (SST-thermistor chain)	Average	**0.54**	-0.03	0.11	0.19
	Median	**0.62**	0.15	0.07	0.37
	Standard deviation	1.12	**1.55**	1.01	1.25
	Minimum	-1.75	**-2.92**	-2.70	-2.92
	Maximum	**3.09**	2.9	1.55	3.09
	Count	18	19	21	58

It is known that the results of remote sensing are applicable to the upper thin layer of water (skin-layer), with a thickness of 10-100 μm. And this temperature differs from the surface temperature in the oceanographic point of view due to the fact that most SST in situ measurements are made at a depth of up to one meter (Siegel et al. 2008) The thermistor chain measurements on the OIFP D-6 were obtained at a depth of several decimeters to one meter depending on the state of the sea surface and sea level anomaly. However, the Table 1 shows that the absolute value of the difference between satellite data and contact measurements did not exceed 3.09 °C, and statistical indicators reflecting the central value of the data set were less than half a degree Celsius (0.19 °C for the average and 0.37 °C for the median). All other things being constant, the Aqua satellite showed the worst results, the Terra satellite has quite good results. The Suomi satellite proved to be the best of all; its standard deviation of the difference between SST and thermistor chain measurements was 1.5 times less than Terra's one. It is impossible to assert with confidence that this fact is related to the difference in the used spectroradiometers (MODIS and VIIRS). Probably, such results were provided with a higher spatial resolution of VIIRS than other devices. The average deviation of this satellite from the location of the D-6 platform was 0.51 km. It is interesting that due to the location of the track of the Terra satellite relative to the OIFP, its average deviation from the point of contact measurements was less than its spatial resolution (Table 1).

The Fig. 8 showed the comparison of the remote sensing data and the in-situ measured temperature values. The one minute time resolution of the thermistor chain allowed making the intercomparison with such time resolution. As can be seen from Fig. 8, most of the values of the two data

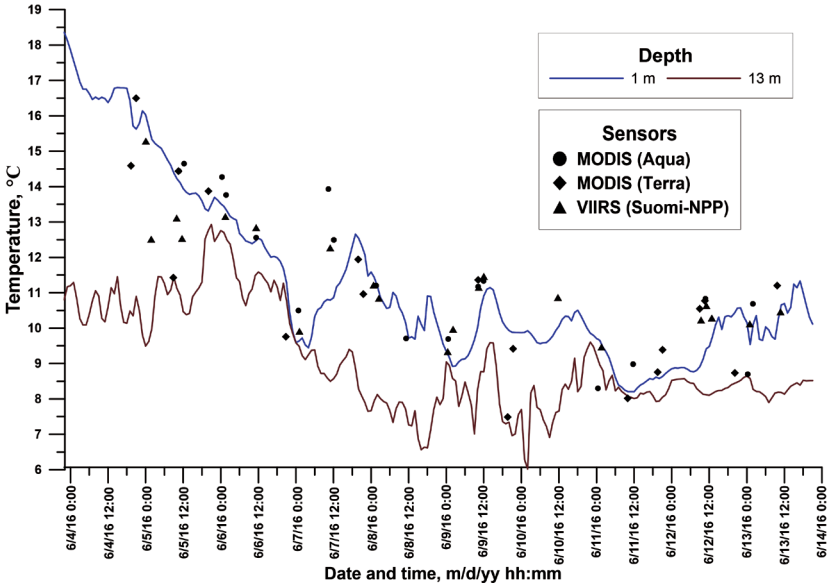

Fig. 8. The comparison of the SST data and the temperature values were obtained by the thermistor chain

samples coincide within about 1 ºC. These results should be recognized as quite good in view of the fact that the satellite acquisition results for this period were obtained under conditions of the thermal structure variability of surface waters, the variable wind speed and sea-surface conditions. All of these are negative physical effects that could create strong differences between the thermal skin-layer and the depth of several decimeters (Robinson 2004).

The intercomparison of SST maps and the thermistor chain measurements demonstrates that despite the representativeness of satellite data for a thin skin-layer, remote sensing data could be used for the surface layer temperature estimation. Due to the fact that satellite imagery shows the dynamics of the processes in general, these data could also be used to study the variability of the temperature of the upper part of UML on a scale exceeding the diurnal one. The lack of data on cloudy days and the long acquisition event interval do not allow to make the analysis of high-frequency temperature variability.

CONCLUSIONS

Based on satellite data, ship measurements and thermistor chain observation the characteristics and dynamics of the sharp decrease in water temperature registered during June 5-12, 2016 in south-eastern Baltic Sea (Gdansk Bay area) are considered. This event led to the considerable SST drop by more than 8 °C for two days. The temperature decreasing caused by the simultaneous action of at least two factors: wind-driven Ekman upwelling and advection of cold water. The temperature decreasing has an impulse character and included several phases. In first phase it was a strong north-north-easterly wind within 2 days which caused Ekman upwelling. A clear response of the temperature to a change in the wind stress was fixed through to the thermistor chain data. In the second phase it was no coastal upwelling, but rather the advection of a cold water stream from the neighbour water areas. All this phases was occurrence in the SST field of the coastal zone arises with the beginning of the first phase and is preserved until the end of the last one. The rate of reduction of its temperature during certain upwelling periods can reach 0.3-0.4 ºC per hour, but the maximum warm-

ing rate between phases varies from 0.25 to 0.28 ºC per hour.

At depths of 30-50 m, the compensatory rise of cold waters leads to the rising of the seasonal thermocline and causes a reduction of the vertical temperature gradients in its core by 2-3 times. This process promotes vertical mixing, as well as the formation of frontal zones in the coastal waters. The movement of cold water offshore by means of Ekman transport ensures their advection to the open sea, reducing the temperature of its surface. So during the upwelling observed from 5 to 12 June 2016 the surface layer temperature in the open sea in the study area dropped by 3-4 °C. In the vicinity of the D-6 platform, the maximum SST amplitude reached 10.22 °C.

An important result of this study is the high correlation between water temperature variability and changes in wind parameters: when the wind speed has decreased and its direction has changed, the response of the vertical thermal structure has occurred very quickly, sometimes within 1 hour. Such a situation was observed during the period of Ekman upwelling occurrence, but during the periods of advection occurrence such feature was not traced. It is impossible to identify such associations using the remote sensing data, due to the limitations caused by the orbital characteristics of the satellites and the large temporal resolution of the data.

However, one should not consider the thermistor chain as a universal tool for studying the coastal upwelling events that could replace satellite data or other devices and methods of in-situ measurements. But the thermistor chain using allows us to look inside the phenomenon and study its vertical structure and small-scale processes. It makes possible to supplement the existing ideas about temperature variability and correctly interpret the measurement results. At the same time, the coastal upwelling is a multifactorial process and for its study and analysis, an integrated approach is required which allow making the simultaneous observation of the same event on different spatial and temporal scales. That is why the simultaneous using of the remote sensing data which illustrate the dynamics of the coastal upwelling over a large area and measurements with a high resolution is important. There is the same situation with meteorological data. It's necessary to have simultaneous measurements of the thermistor chain and the weather station for the understanding of the processes occurring within the upwelling phenomenon and their cause-and-effect relationship. At the same time, the reanalysis data show us the meteorological situation in the entire water area of the study area and beyond. Of course, for a correct comprehensive analysis of the upwelling process and its origin, it is necessary to observe the currents. The absence of such data in the presented study is undoubtedly a negative fact. It is also very promising to continue research in this area is the usage of three moored thermistor chains, located in the shape of a triangle at a distance of several kilometres from each other. This modification will make it possible to observe the processes of water advection along and across the shelf, as well as a vertical structure variability during upwelling events more better.

ACKNOWLEDGEMENTS

This research was performed in the framework of the state assignment of IO RAS (Theme No.0149-2019-0013). The part of work in analysis thermos-chain data were obtained within the RSF grant (project No.14-50-00095). Authors are grateful to LLC "Lukoil-KMN" (Kaliningrad) for assistance in the installation of equipment and organization of data acquisition process.

REFERENCES

Ambrosimov A.K., Kabatchenko I.M., Stont Z.I., Yakubov S.K. (2013) Seasonal characteristics of waves in the southeastern part of the Baltic Sea in 2008-2009. Russian Meteorology and Hydrology, 38, (3), pp. 191-198. DOI:10.3103/S1068373913030084.

Brookes J.D., O'Brien K.R., Burford M.A., Bruesewitz D.A., Hodges B.R., McBride C., and Hamilton D.P. (2013). Effects of diurnal vertical mixing and stratification on phytoplankton productivity in geothermal Lake Rotowhero, New Zealand. Inland Waters, 3(3), 369-376. DOI: 10.5268/IW-3.3.625

Bychkova I.A., Viktorov S.V., Shumakher D.A. (1988). A relationship between the large-scale atmospheric circulation and the origin of coastal upwelling in the Baltic Sea. Russian Meteorology and Hydrology, 10, pp. 91–98 (in Russian).

Bychkova I. and Viktorov S. (1987). Use of satellite data for identification and classification of upwelling in the Baltic Sea. Oceanology, 27(2), pp. 158-162.

Chubarenko I.P., Afonov V.V., Chugaevich V.Ya., Krechik V.A. (2013). Water dynamics above the sloping bottom due to an intense summer heating. Russian Meteorology and Hydrology, 1, pp. 66-78. DOI:10.3103/S1068373913010068.

CISL Research Data Archive (2018). NCEP/NCAR Reanalysis Project. [online] Available at: http://rda.ucar.edu/ [Accessed 26 Oct. 2018].

Demchenko N.Yu. and Chubarenko I.P. (2012). Spatiotemporal variability of thermal front features in the Baltic Sea 2010-2011. Oceanology, №6 (52), pp. 790-797. DOI:10.1134/S0001437012060021.

Demidov A.N., Myslenkov S.A., Gritsenko V.A., Chugaevich V.Ya., Sultanov P.A., Pisareva M.N., Silvestrova K.P., Polukhin A.A. (2011). Specific features of water structure and dynamics within the coastal part of the Baltic Sea near the Sambian Peninsula. Moscow State University Bulletin. Series 5. Geography, 1, pp. 41–47 (in Russian with English summary).

Elachi Ch., and Jakob J. Van Zyl (2006). Introduction To The Physics and Techniques of Remote Sensing, 2nd Edition. John Wiley & Sons. DOI:10.1063/1.2811643.

Esiukova E.E., Chubarenko I.P., Stont Zh.I. (2017). Upwelling or differential cooling? Analysis of satellite SST images of the Southeastern Baltic Sea. Water Resources, 44 (1), pp. 69-77. DOI:10.1134/s0097807817010043.

Gemmrich J.R. and Van Haren H. (2001). Thermal fronts generated by internal waves propagating obliquely along the continental slope. Journal of physical oceanography, 31(3), 649-655. DOI: 10.1175/1520-0485(2001)031<0649:TFGBIW>2.0.CO;2

Gemmrich J.R. and Van Haren H. (2002). Internal wave band eddy fluxes above a continental slope. Journal of marine research, 60(2), 227-253. DOI: 10.1357/00222400260497471

Gidhagen L. (1987). Coastal upwelling in the Baltic Sea—Satellite and in situ measurements of sea-Surface temperatures indicating coastal upwelling. Estuarine, Coastal and Shelf Science, 24 (4), pp. 449–62. DOI:10.1016/0272-7714(87)90127-2.

Hela I. (1976). Vertical velocity of the upwelling in the sea. Commentationes physico-mathematicae, 46(1), pp. 9-24.

Horstmann U. (1983). Distribution patterns of temperature and water colour in the Baltic Sea as recorded in satellite images: indicators for phytoplankton growth. Kiel: Institut für Meereskunde an der Universität Kiel. DOI:10.3289/ifm_ber_106.

Kahru M., Håkansson B., Rud O. (1995). Distributions of the sea-Surface temperature fronts in the Baltic Sea as derived from satellite imagery. Continental Shelf Research, 15 (6), pp. 663–79. DOI:10.1016/0278-4343(94)e0030-p.

Kapustina M.V., Krechik V.A., Gritsenko V.A. (2017). Seasonal variations in the vertical structure of temperature and salinity fields in the shallow Baltic Sea off the Kaliningrad region coast. Russian Journal of Earth Sciences, 17 (1). pp. 1-7. DOI: 10.2205/2017ES000595.

Kowalewski M. and Ostrowski M. (2005). Coastal up- and downwelling in the southern Baltic. Oceanologia, 47(4), pp. 435-475.

Kozlov I.E., Kudryavtsev V.N., Johannessen J.A., Chapron B., Dailidienė I., Myasoedov A.G. (2012). ASAR imaging for coastal upwelling in the Baltic Sea. Advances in Space Research, 50 (8), pp. 1125-137. DOI:10.1016/j.asr.2011.08.017.

Krechik V.A. and Gritsenko V.A. (2016). Thermal structure of the coastal waters of the Baltic sea near the north coast of the Kaliningrad region. Processes in Geomedia, 5, pp. 77-84 (in Russian with English summary).

Krężel A., Ostrowksi M., Szymelfenig M. (2005). Sea surface temperature distribution during upwelling along the Polish Baltic coast. Oceanologia, 47(4), pp. 415-432.

Lehmann A. and Myrberg K. (2008). Upwelling in the Baltic Sea-A review. Journal of Marine Systems, 74, pp. 3-12. DOI:10.1016/j.jmarsys.02.010.

Lehmann A., Myrberg K., Höflich K. (2012). A statistical approach to coastal upwelling in the Baltic Sea based on the analysis of satellite data for 1990–2009. Oceanologia, 54 (3), pp. 369-93. DOI:10.5697/oc.54-3.369.

Lehmann R. (2013). 3 σ-Rule for Outlier Detection from the Viewpoint of Geodetic Adjustment. Journal of Surveying Engineering, 139(4), 157-165. DOI: 10.1061/(ASCE) SU.1943-5428.0000112.

Leppäranta M. and Myrberg K. (2010) Physical oceanography of the Baltic Sea. Chichester, U.K.: Springer/Praxis Pub. DOI:10.1007/978-3-662-04453-7_2.

Massel S.R. (2015). Internal Gravity Waves in the Shallow Seas. GeoPlanet: Earth and Planetary Sciences. Springer Int. Publ, Switzerland. DOI:10.1007/978-3-319-18908-6.

Morozov Ye.G., Shchuka C.A., Zapotylko V.S. (2007). Towed spectra of internal waves on a pycnocline in the Baltic. Doklady Earth Sciences, 412 (4), pp. 552-554. (in Russian with English summary).

Myslenkov S.A., Krechik V.A., Bondar A.V. (2017a). Daily and seasonal water temperature changes in the coastal zone of the Baltic Sea measured by thermistor chain. Ecological Systems and Devices, 5, pp. 25–33. (in Russian with English summary).

Myslenkov S.A., Krechik V.A., Soloviev D.M. (2017b). Water temperature analysis in the coastal zone of the Baltic Sea based on thermistor chain observations and satellite data. Proceedings of Hydrometcentre of Russia, 364, pp. 159–169 (in Russian with English summary).

Pukelsheim F. (1994). The three sigma rule. The American Statistician, 48(2), 88-91. DOI:10.1080/00031305.1994.10476030.

Robinson I.S. (2004). Measuring Ocean from Space: The Principals and Methods of Satellite Oceanography. Springer,Berlin, 668 pp.

Saha S., Moorthi S., Wu X., Wang J., Nadiga S., Tripp P., Behringer D., Hou Y., Chuang H., Iredell M., Ek M., Meng J., Yang R., Mendez M.P., van den Dool H., Zhang Q., Wang W., Chen M., Becker E. (2014). The NCEP Climate Forecast System Version 2. J. Climate, 27, pp. 2185–2208. DOI:10.1175/JCLI-D-12-00823.1

Sellschopp J. (1991). Stochastic ray tracing in thermoclines. In Ocean Variability & Acoustic Propagation (pp. 293-312). Springer, Dordrecht. DOI: 10.1007/978-94-011-3312-8_23

Serebryany A.N. and Khymchenko E.E. (2014). Observations of internal waves at Caucasian and Crimean shelves of the Black Sea in summer 2013. Current problems in remote sensing of the Earth from space, 11 (3), pp. 88-104. (in Russian with English summary).

Siegel H., Gerth M., Neumann T., Doerffer R. (1999). Case studies on phytoplankton blooms in coastal and open waters of the Baltic Sea using Coastal Zone Color Scanner data. International Journal of Remote Sensing, 20 (7), pp. 1249-1264. DOI:10.1080/014311699212713.

Siegel H., Gerth M., Tschersich G. (2008). Satellite–Derived Sea Surface Temperature for the Period 1990–2005. State and Evolution of the Baltic Sea, 1952–2005: A Detailed 50–Year Survey of Meteorology and Climate, Physics, Chemistry, Biology, and Marine Environment. pp. 241-264.

Simons T.J. (1978). Wind-driven circulations in the southwest Baltic. Tellus, 30 (3), pp. 272-83. DOI:10.3402/tellusa.v30i3.10341.

Sivkov V.V., Kadzhoyan Yu.S., Pichuzhkina O.Ye., Feldman V.N. (2012). Oil and environment of the Kaliningrad region. Kaliningrad: Terra Baltika. (in Russian).

Stepanova N.B., Shchuka S.A., Chubarenko I.P. (2015). Structure and evolution of the cold intermediate layer in the southeastern part of the Baltic sea by the field measurement data of 2004-2008. Oceanology, 55, (1), pp. 25-35. DOI:10.1134/S0001437015010154.

Stont Zh.I., Gushchin O.A., Dubravin V.F. (2012). Storm winds in the southeast Baltic according to the data of the automatic meteorological station in 2004-2010. Proceedings of the Russian Geographical Society, 144 (1), pp. 51-58. (in Russian with English summary).

Svansson A. (1975). Interaction between the coastal zone and the open sea. Finnish marine research, 239, pp. 11–28.

Van der Lee E.M. and Umlauf L. (2011). Internal wave mixing in the Baltic Sea: Near–inertial waves in the absence of tides. Journal of Geophysical Research: Oceans, 116(C10). DOI: 10.1029/2011JC007072.

Van Haren H., Groenewegen R., Laan M., Koster B. (2005). High sampling rate thermistor string observations at the slope of Great Meteor Seamount. Ocean Science, 1(1), 17-28. DOI: 10.5194/os-1-17-2005.

Walin G. (1972). Some observations of temperature fluctuations in the coastal region of the Baltic. Tellus, 24 (3), pp. 187-98. DOI:10.3402/tellusa.v24i3.10633.

Zhelezova E., Krek E., Chubarenko B. (2018) Characteristics of the polynya in the Vistula Lagoon of the Baltic Sea by remote sensing data. International Journal of Remote Sensing, [online], pp. 1-12. Available at: https://www.tandfonline.com/doi/abs/10.1080/01431161.2018.1524181. DOI: 10.1080/01431161.2018.1524181.

Zhurbas V., Elken J., Paka V., Piechura J., Väli G., Chubarenko I., Golenko N., Shchuka S. (2012). Structure of unsteady overflow in the Slupsk furrow of the Baltic Sea. Journal of Geophysical Research, 117 (C4), pp. C04027. DOI:10.1029/2011JC007284.

Received on November 16th, 2018 Accepted on February 20th, 2019